Proceedings of the 2001 IEEE
International Conference on Robotics & Automation
Seoul, Korea • May 21-26, 2001

Learning a Coordinate Transformation for a Human Visual Feedback Controller based on Disturbance Noise and the Feedback Error Signal

Eimei Oyama and Nak Young Chong
National Institute of Advanced Industrial Science and Technology
Namiki 1-2, Tsukuba-shi, Ibaraki
305-8564 Japan
eimei@mel.go.jp

Arvin Agah
Dept. of Electrical Engineering and Computer Science
The University of Kansas
Lawrence, KS 66045 USA

Taro Maeda and Susumu Tachi
School of Engineering
The University of Tokyo
Hongo 7-3-1, Bunkyo-ku
Tokyo 113-8656 Japan

Karl F. MacDorman
Dept. of Systems and Human Science
Graduate School of Engineering Science
Osaka University
Toyonaka, Osaka 560-8531 Japan

Abstract

The speed, accuracy, and adaptability of human movement depends on the brain performing an inverse kinematics transformation — that is, a transformation from visual to joint angle coordinates — based on learning from experience. In human motion control, it is important to learn a feedback controller for the hand position error in the human inverse kinematics solver. This paper proposes a novel model that uses disturbance noise and the feedback error signal to learn coordinate transformations of the human visual feedback controller. The proposed model redresses drawbacks in current models because it does not rely on complex signal switching, which does not seem neurophysiologically plausible. Numerical simulations show the effectiveness of the model.

1 Introduction

The task of calculating each joint angle that would result in a specific hand position in the visual coordinates is called the inverse kinematics problem. An infant without a thumb had a major surgical operation, transplanting an index finger as a thumb, which is kinematically influential. After the operation, the child was able to learn how to use the index finger like a thumb [1]. The angle between an index finger and a thumb is about 90 degrees when we do some tasks using the fingers. If the coordinate transformation of the visual feedback controller is fixed, the total hand position controller probably cannot adapt 90 degrees change. We believe that the coordinate transformation learning is necessary to explain the motor learning capability of humans. Although a number of learning models of the visual feedback controller have been proposed [2][3][4], a definitive learning model has not yet been obtained.

Many researchers [2][4] employ *direct inverse modeling*. However, it requires the complex switching of the input signal to the inverse model from the *desired* hand position, velocity, or acceleration during hand position control to the *observed* hand position, velocity, or acceleration during inverse model learning. Although the desired and observed signal might coincide, their characteristics are quite different. No research has yet modeled the switching system successfully. Furthermore, the learning model is not "goal-directed": there is no direct way of finding an action that corresponds to a particular desired result [3]. The *forward and inverse modeling* proposed by Jordan [3] requires a back-propagation signal; this technique lacks a biological basis [5]. It also requires complex switching of the desired *output* signal of the forward model from the *observed* hand position during forward model learning to the *desired* hand position during the learning of the inverse kinematics solver. We believe that the complex signal switching for the learning required by *direct inverse modeling* or *forward and in-*

verse modeling does not occur in the relatively low-level sensorimotor learning of the human nervous system. The *feedback error learning* proposed by Kawato [6] requires a pre-existing accurate feedback controller.

We would like our learning model to be *(1)* relatively simple, *(2)* biologically plausible, and *(3)* to cover the behavioral data. We have already proposed two models for learning the coordinate transformation function of the hand position feedback controller. One of the models is based on disturbance noise in the hand position control loop [7]. The other is based on changes in hand position error [8]. Both can avoid complex signal switching. However, since the former model becomes inaccurate when the disturbance noise is infinitesimal, we propose a new learning model of the position feedback controller based on disturbance noise and the feedback error signal [9][10]. Although the learning based on the feedback error signal is effective only if the feedback controller is reasonably accurate, the learning based on disturbance noise during the initial stage of the learning can obtain the accurate status of the controller. The feedback error signal by the accurate controller can keep the coordinate transformation function of the controller in the cases that the disturbance noise is infinitesimal. Since the two learning signals complement each other, the performance of the novel learning model is much improved.

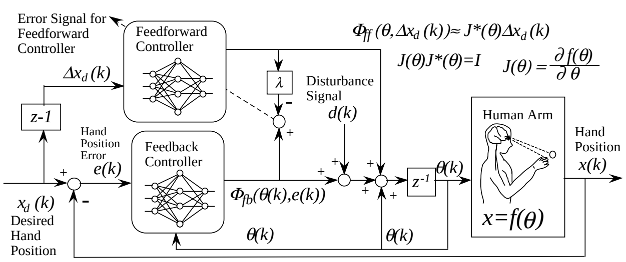

Fig. 1: Configuration of 1-st Order Model of Hand Position Controller

2 Background

2.1 Hybrid Inverse Kinematics Solver

Before proposing the model for learning the hand position feedback controller, we state the model of the human inverse kinematics solver. Let $\boldsymbol{\theta} \in \mathbf{R}^m$ be the joint angle vector and $\boldsymbol{x} \in \mathbf{R}^n$ be the hand position/orientation vector given by the vision system. The relationship between $\boldsymbol{x}$ and $\boldsymbol{\theta}$ is expressed as $\boldsymbol{x} = \boldsymbol{f}(\boldsymbol{\theta})$ where f is a C^1 class function. The Jacobian of the hand position vector is expressed as $\boldsymbol{J}(\boldsymbol{\theta}) = \partial \boldsymbol{f}(\boldsymbol{\theta})/\partial \boldsymbol{\theta}$. Let $\boldsymbol{x}_d(k)(k = -\gamma T, -\gamma T + 1, \dots, -1, 0, 1, 2, \dots, T-1, T)$ be the desired hand position and $\boldsymbol{e}(k) = \boldsymbol{x}_d(k) - \boldsymbol{x}(k) = \boldsymbol{x}_d(k) - \boldsymbol{f}(\boldsymbol{\theta}(k))$ be the hand position error vector. γ is an appropriate constant which can make γT an integer. We assume that $\boldsymbol{x}_d(k) = \boldsymbol{x}_d(0)$, $\boldsymbol{e}(k) = \boldsymbol{0}$ and $\boldsymbol{\theta}(k) = \boldsymbol{\theta}(0)$ are established when $k \leq 0$. The hybrid control system, consisting of a learning feedback controller and a learning feed-forward controller, is considered.

The feed-forward controller $\boldsymbol{\Phi}_{ff}(\boldsymbol{\theta}(k), \boldsymbol{\Delta x}_d(k)) \in \mathbf{R}^m$ transforms the change of the desired hand position $\boldsymbol{\Delta x}_d(k) = \boldsymbol{x}_d(k+1) - \boldsymbol{x}_d(k)$ to the joint angle vector space. The feedback controller $\boldsymbol{\Phi}_{fb}(\boldsymbol{\theta}(k), \boldsymbol{e}(k)) \in \mathbf{R}^m$ transforms the hand position error $\boldsymbol{e}(k)$ to the joint angle vector space. The following first order control system is considered:

$$\boldsymbol{\theta}(k+1) = \boldsymbol{\theta}(k) + \boldsymbol{\Delta\theta}(k) \tag{1}$$

$$\boldsymbol{\Delta\theta}(k) = \boldsymbol{d}(k) + \boldsymbol{\Delta\theta}_c(k) \tag{2}$$

$$\begin{aligned}\boldsymbol{\Delta\theta}_c(k) = {} & \boldsymbol{\Phi}_{ff}(\boldsymbol{\theta}(k), \boldsymbol{\Delta x}_d(k)) \\ & + \boldsymbol{\Phi}_{fb}(\boldsymbol{\theta}(k), \boldsymbol{e}(k))\end{aligned} \tag{3}$$

where $\boldsymbol{d}(k)$ is assumed to be a disturbance noise from all components except the hand position control system. We assume that $\boldsymbol{d}(k)$ has no correlation with the change of the desired hand position $\boldsymbol{\Delta x}_d(k)$. Let $\boldsymbol{R}_d$ be the covariance matrix of $\boldsymbol{d}(k)$ defined as

$$\boldsymbol{R}_d = E[\boldsymbol{d}(k)\boldsymbol{d}^T(k)] \tag{4}$$

where $E[\boldsymbol{t}]$ is the expected value of a scalar, a vector, or a matrix function $\boldsymbol{t}$.

We have already proposed the learning model based on the disturbance noise in the hand position control loop [7]. There are a variety of sources of the disturbance noise in human motion control. *(1)* Infants experience various kinds of motions including reflexes before they can reach and grasp objects [11][12]. Motion signals that are not generated by the hand position controller can be regarded as disturbance noise. *(2)* Based on observations of motor-neural firing [13][14], Harris and Wolpert assumed that the neural control signal contains noise that increases with the mean of the signal [15]. *(3)* Nakamura uses the excitatory spikes from thalamic neurons to the cerebral cortex to generate the random motions in his reinforcement learning models [16]. *(4)* A lack of completeness in the inverse dynamics solver can cause the desired and real joint motion to differ. The error can be regarded as disturbance noise. The physiological tremor [17] may be an example of this.

Fig. 1 shows the configuration of the hybrid control system. In this figure, z^{-1} is the operator that indicates a one-step delay in the discrete time signal by a sampling interval of Δt, and $z-1$ is the operator that calculates the change in the signal. Although the human hand position control system includes higher order complex dynamics terms which are ignored in Equation (3), McRuer's experimental model of human compensation control suggests that the term that converts the hand position error to the hand velocity is a major term in the human control system [18]. We consider Equation (3) to be a good approximate model for the analysis of coordinate transformation learning in humans.

The learner $\boldsymbol{\Phi}_{fb}(\boldsymbol{\theta}, \boldsymbol{e})$, and the learner $\boldsymbol{\Phi}_{fb}(\boldsymbol{\theta}, \boldsymbol{e})$ are modeled using an artificial neural network. Let $\boldsymbol{\Phi}'_{fb}(\boldsymbol{\theta}, \boldsymbol{e})$ be the desired output of the learner $\boldsymbol{\Phi}_{fb}(\boldsymbol{\theta}, \boldsymbol{e})$ and $\boldsymbol{\Phi}'_{ff}(\boldsymbol{\theta}, \boldsymbol{\Delta x}_d)$ be the desired output of the learner $\boldsymbol{\Phi}_{ff}(\boldsymbol{\theta}, \boldsymbol{\Delta x}_d)$. $\boldsymbol{\Phi}'_{fb}(\boldsymbol{\theta}, \boldsymbol{e})$ and $\boldsymbol{\Phi}'_{ff}(\boldsymbol{\theta}, \boldsymbol{\Delta x}_d)$ function as teachers for $\boldsymbol{\Phi}_{fb}(\boldsymbol{\theta}, \boldsymbol{e})$ and $\boldsymbol{\Phi}_{ff}(\boldsymbol{\theta}, \boldsymbol{\Delta x}_d)$, respectively. Without any prior knowledge of the function $\boldsymbol{f}(\boldsymbol{\theta})$, or the Jacobian $\boldsymbol{J}(\boldsymbol{\theta})$, we examine how to learn a hand position controller by observing the hand position $\boldsymbol{x}(k)$ and the joint angle vector $\boldsymbol{\theta}(k)$ only.

2.2 Feed-forward Controller Learning

According to Kawato's *feedback error learning* [6], we use $\boldsymbol{\Phi}'_{ff}(\boldsymbol{\theta}(k), \boldsymbol{\Delta x}_d(k))$ expressed as:

$$\begin{aligned}&\boldsymbol{\Phi}'_{ff}(\boldsymbol{\theta}(k-1), \boldsymbol{\Delta x}_d(k-1))\\&= (1-\lambda)\boldsymbol{\Phi}_{ff}(\boldsymbol{\theta}(k-1), \boldsymbol{\Delta x}_d(k-1))\\&\quad + \boldsymbol{d}(k-1) + \boldsymbol{\Phi}_{fb}(\boldsymbol{\theta}(k), \boldsymbol{e}(k))\end{aligned} \tag{5}$$

where λ is a small, positive, real number for stabilizing the learning process and ensuring that equation $\boldsymbol{\Phi}_{ff}(\boldsymbol{\theta}, \boldsymbol{0}) \approx \boldsymbol{0}$ holds. The second term on the right-hand side of Equation (5), $\boldsymbol{d}(k-1)$, is used to compensate the influence of the disturbance noise $\boldsymbol{d}(k-1)$ included by $\boldsymbol{e}(k)$. We call the following term the modified feedback error signal.

$$\boldsymbol{\Phi}^*_{fb}(\boldsymbol{\theta}(k), \boldsymbol{e}(k)) = \boldsymbol{\Phi}_{fb}(\boldsymbol{\theta}(k), \boldsymbol{e}(k)) + \boldsymbol{d}(k-1). \tag{6}$$

If the joint angle vector changes according to Equation (1) and $\boldsymbol{\Delta\theta}(k-1)$ is small enough, the change of the hand position is approximated as follows:

$$\begin{aligned}\boldsymbol{\Delta x}(k-1) &= \boldsymbol{f}(\boldsymbol{\theta}(k)) - \boldsymbol{f}(\boldsymbol{\theta}(k-1))\\&\approx \boldsymbol{J}(\boldsymbol{\theta}(k-1))\boldsymbol{\Delta\theta}(k-1).\end{aligned} \tag{7}$$

The updated hand position error $\boldsymbol{e}(k+1)$ is approximated by

$$\boldsymbol{e}(k+1) = \boldsymbol{e}(k) + \boldsymbol{\Delta x}_d(k) - \boldsymbol{\Delta x}(k)$$

$$\approx \boldsymbol{e}_{fb}(k) + \boldsymbol{e}_{ff}(k) - \boldsymbol{J}(\boldsymbol{\theta})\boldsymbol{d}(k-1) \tag{8}$$

$$\boldsymbol{e}_{fb}(k) = \boldsymbol{e}(k) - \boldsymbol{J}(\boldsymbol{\theta}(k))\boldsymbol{\Phi}_{fb}(\boldsymbol{\theta}(k), \boldsymbol{e}(k)) \tag{9}$$

$$\boldsymbol{e}_{ff}(k) = \boldsymbol{\Delta x}_d(k) - \boldsymbol{J}(\boldsymbol{\theta}(k))\boldsymbol{\Phi}_{ff}(\boldsymbol{\theta}(k), \boldsymbol{\Delta x}_d(k)). \tag{10}$$

When $\boldsymbol{\Psi}_{fb}(\boldsymbol{\theta})$ is an appropriate coordinate transformation gain of the feedback controller, the error signal for the feed-forward controller $\boldsymbol{\Delta\Phi}_{ff}(\boldsymbol{\theta}, \boldsymbol{\Delta x}_d) = \boldsymbol{\Phi}'_{ff}(\boldsymbol{\theta}, \boldsymbol{\Delta x}_d) - \boldsymbol{\Phi}_{ff}(\boldsymbol{\theta}, \boldsymbol{\Delta x}_d)$ can be approximated as:

$$\begin{aligned}&\boldsymbol{\Delta\Phi}_{ff}(\boldsymbol{\theta}(k-1), \boldsymbol{\Delta x}_d(k-1))\\&\approx -\lambda\boldsymbol{\Phi}_{ff}(\boldsymbol{\theta}(k-1), \boldsymbol{\Delta x}_d(k-1))\\&\quad + \boldsymbol{\Psi}_{fb}(\boldsymbol{\theta})\boldsymbol{e}_{fb}(k-1) + \boldsymbol{\Psi}_{fb}(\boldsymbol{\theta})\boldsymbol{e}_{ff}(k-1)\\&\quad + (\boldsymbol{I}_m - \boldsymbol{\Psi}_{fb}(\boldsymbol{\theta})\boldsymbol{J}(\boldsymbol{\theta}))\boldsymbol{d}(k-1).\end{aligned} \tag{11}$$

The feed-forward controller is updated by the above error signal. The third term on the right-hand side of Equation (11) can reduce the error of the feed-forward controller $\boldsymbol{e}_{ff} = \boldsymbol{\Delta x}_d - \boldsymbol{J}(\boldsymbol{\theta})\boldsymbol{\Phi}_{ff}(\boldsymbol{\theta}, \boldsymbol{\Delta x}_d)$. The learning result $\boldsymbol{J}(\boldsymbol{\theta})\boldsymbol{\Phi}_{ff}(\boldsymbol{\theta}, \boldsymbol{\Delta x}_d) \approx \boldsymbol{\Delta x}_d$ is obtained. Section 4 show its derivation.

3 A Novel Learning Model for the Feedback Controller

3.1 Feedback Controller Learning by Disturbance Noise

We proposed the learning model of the human inverse kinematics solver based on the assumption that the feedback controller tries to compensate for the disturbance noise in the control loop [7]. If the output of the feed-forward controller $\boldsymbol{\Phi}_{ff}(\boldsymbol{\theta}(k), \boldsymbol{\Delta x}_d(k))$ and the output of the feedback controller $\boldsymbol{\Phi}_{fb}(\boldsymbol{\theta}(k), \boldsymbol{e}(k))$ is precise enough, $\boldsymbol{e}(k+1) \approx -\boldsymbol{J}(\boldsymbol{\theta}(k))\boldsymbol{d}(k)$ is obtained according to Equation (8). One role of the feedback controller is to compensate for disturbance noise. To compensate for $\boldsymbol{d}(k)$ at time $k+1$, the output of the feedback controller should be $-\boldsymbol{d}(k)$. The proposed learning model based on the disturbance noise can be expressed by

$$\boldsymbol{\Phi}'_{fb}(\boldsymbol{\theta}(k), \boldsymbol{e}(k)) = -\boldsymbol{d}(k-1). \tag{12}$$

The error signal for the hand position feedback controller $\boldsymbol{\Delta\Phi}_{fb}(\boldsymbol{\theta}, \boldsymbol{e}) = \boldsymbol{\Phi}'_{fb}(\boldsymbol{\theta}, \boldsymbol{e}) - \boldsymbol{\Phi}_{fb}(\boldsymbol{\theta}, \boldsymbol{e})$ can expressed as follows:

$$\begin{aligned}&\boldsymbol{\Delta\Phi}_{fb}(\boldsymbol{\theta}(k), \boldsymbol{e}(k)) = -\boldsymbol{d}(k-1) - \boldsymbol{\Phi}_{fb}(\boldsymbol{\theta}(k), \boldsymbol{e}(k))\\&= -\boldsymbol{\Phi}^*_{fb}(\boldsymbol{\theta}(k), \boldsymbol{e}(k)).\end{aligned} \tag{13}$$

The feedback controller is updated by the above error signal. The right-hand side of Equation (13) is the product of a negative sign and the modified feedback error signal. Fig. 2 shows the conceptual diagram of the learning model (12). The dotted line shows the error signal for learning the feedback controller. The learning result is expressed by

$$\boldsymbol{\Phi}_{fb}(\boldsymbol{\theta}, \boldsymbol{e}) \approx \boldsymbol{J}^+(\boldsymbol{\theta})\boldsymbol{e} \tag{14}$$

$$\boldsymbol{J}^+(\boldsymbol{\theta}) = \boldsymbol{R}_d\boldsymbol{J}^T(\boldsymbol{\theta})(\boldsymbol{J}(\boldsymbol{\theta})\boldsymbol{R}_d\boldsymbol{J}^T(\boldsymbol{\theta}))^{-1}. \tag{15}$$

$\boldsymbol{J}^+(\boldsymbol{\theta})$ is the pseudo-inverse matrix (Moore-Penrose's generalized inverse matrix) of $\boldsymbol{J}(\boldsymbol{\theta})$. The derivation of the above result will be illustrated in Section 4. The feedback controller expressed in Equation (14) can appropriately perform the coordinate transformation from visual to joint angle coordinates.

After learning the feedback controller, $\boldsymbol{d}(k)$ should be small enough to control the hand precisely. However, when $\boldsymbol{d}(k)$ is $\mathbf{0}$, $\boldsymbol{\Phi}_{fb}(\boldsymbol{\theta}, \boldsymbol{e})$ slowly converges on $\mathbf{0}$ by the learning rule (12). To avoid this drawback, we will exploit *feedback error learning* [6] for the learning of the feedback controller.

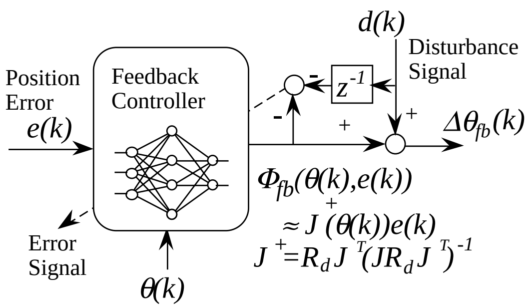

Fig. 2: Learning based on Disturbance Noise

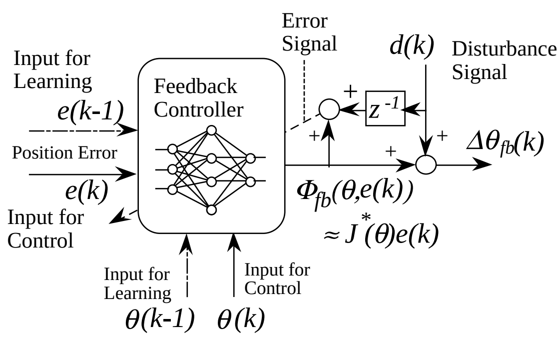

Fig. 3: Learning based on Feedback Error Signal

3.2 Feedback Controller Learning by Feedback Error Learning

We can use the feedback error signal for learning the feedback controller, as well as the feed-forward controller, given by

$$\boldsymbol{\Phi}'_{fb}(\boldsymbol{\theta}(k-1), \boldsymbol{e}(k-1)) = \boldsymbol{\Phi}_{fb}(\boldsymbol{\theta}(k-1), \boldsymbol{e}(k-1)) + \boldsymbol{\Phi}^*_{fb}(\boldsymbol{\theta}(k), \boldsymbol{e}(k)). \quad (16)$$

Fig. 3 shows the conceptual diagram of the learning model (16).

The error signal for the feedback controller is expressed as follows:

$$\boldsymbol{\Delta\Phi}_{fb}(\boldsymbol{\theta}(k-1), \boldsymbol{e}(k-1)) = \boldsymbol{\Phi}^*_{fb}(\boldsymbol{\theta}(k), \boldsymbol{e}(k)). \quad (17)$$

$\boldsymbol{\Delta\Phi}_{fb}(\boldsymbol{\theta}, \boldsymbol{e})$ can be approximated as follows:

$$\begin{aligned}&\boldsymbol{\Delta\Phi}_{fb}(\boldsymbol{\theta}(k-1), \boldsymbol{e}(k-1)) \\ &\approx \boldsymbol{\Psi}_{fb}(\boldsymbol{\theta})\boldsymbol{e}_{fb}(k-1) + \boldsymbol{\Psi}_{fb}(\boldsymbol{\theta})\boldsymbol{e}_{ff}(k-1) \\ &\quad + (\boldsymbol{I}_m - \boldsymbol{\Psi}_{fb}(\boldsymbol{\theta})\boldsymbol{J}(\boldsymbol{\theta}))\boldsymbol{d}(k-1). \quad (18)\end{aligned}$$

The first term on the right-hand side of Equation (18) can reduce the error of the feedback controller $\boldsymbol{e}_{fb} = \boldsymbol{e} - \boldsymbol{J}(\boldsymbol{\theta})\boldsymbol{\Phi}_{fb}(\boldsymbol{\theta}, \boldsymbol{e})$. If $\boldsymbol{\Phi}_{fb}(\boldsymbol{\theta}, \boldsymbol{e})$ satisfies $\boldsymbol{\Phi}_{fb}(\boldsymbol{\theta}, \mathbf{0}) = \mathbf{0}$ and the learning is started from a good initial status of the feedback controller, the learning result $\boldsymbol{J}(\boldsymbol{\theta})\boldsymbol{\Phi}_{fb}(\boldsymbol{\theta}, \boldsymbol{e}) \approx \boldsymbol{e}$ is obtained. However, the learning signal based on the *feedback error signal* is effective only if the feedback controller is accurate enough. It is difficult for this learning model to explain the human learning capability.

3.3 Learning based on Disturbance Noise and Feedback Error Signal

The right-hand side of Equation (17) is the product of a negative sign and the right-hand side of Equation (13). The difference of the time of the input signal to $\boldsymbol{\Phi}_{fb}(\boldsymbol{\theta}, \boldsymbol{e})$ produces similar learning results. To explain the human learning function in the cases that the feedback controller is inaccurate and to keep the feedback gain in the cases that the disturbance noise is infinitesimal, the error signals defined in Equation (13) and Equation (17) can be used simultaneously at time k. The proposed novel error signal can be expressed as follows:

$$\begin{aligned}\boldsymbol{\Delta\Phi}_{fb}(\boldsymbol{\theta}(k-1), \boldsymbol{e}(k-1)) &= \boldsymbol{\Phi}^*_{fb}(\boldsymbol{\theta}(k), \boldsymbol{e}(k)) \\ &\quad - \boldsymbol{\Phi}^*_{fb}(\boldsymbol{\theta}(k-1), \boldsymbol{e}(k-1)). \quad (19)\end{aligned}$$

The desired output signal for $\boldsymbol{\Phi}_{fb}(\boldsymbol{\theta}(k-1), \boldsymbol{e}(k-1))$ can be expressed as follows:

$$\begin{aligned}\boldsymbol{\Phi}'_{fb}(\boldsymbol{\theta}(k-1), \boldsymbol{e}(k-1)) &= -\boldsymbol{d}(k-2) \\ &\quad + \boldsymbol{d}(k-1) + \boldsymbol{\Phi}_{fb}(\boldsymbol{\theta}(k), \boldsymbol{e}(k)). \quad (20)\end{aligned}$$

The above signal can be calculated as the linear combination of the control signals. To satisfy $\boldsymbol{\Phi}_{fb}(\boldsymbol{\theta}, \mathbf{0}) \approx \mathbf{0}$, even using a general learner, Equation (20) should be modified as follows:

$$\begin{aligned}\boldsymbol{\Phi}'_{fb}(\boldsymbol{\theta}(k-1), \boldsymbol{e}(k-1)) &= -\boldsymbol{d}(k-2) \\ &\quad + \boldsymbol{d}(k-1) + \boldsymbol{\Phi}_{fb}(\boldsymbol{\theta}(k), \boldsymbol{e}(k)) \\ &\quad - \lambda_{fb}\boldsymbol{\Phi}_{fb}(\boldsymbol{\theta}(k-1), \boldsymbol{e}(k-1)) \quad (21)\end{aligned}$$

where λ_{fb} is a small, positive, real number. Fig. 4 shows the conceptual diagram of the proposed learning model. The learning model is only a little more complex than the models presented in Fig. 2 and Fig. 3.

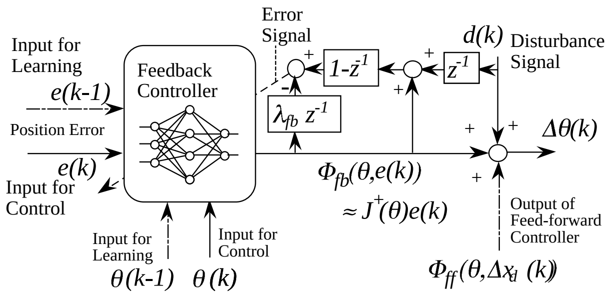

Fig. 4: Learning based on Disturbance Noise and Feedback Error Signal

When $\boldsymbol{d}(k)$ is not $\mathbf{0}$ and λ_{fb} is small enough, we obtain the same learning result as in Equation (14). The derivation of the learning result will be illustrated in Section 4. When $\boldsymbol{d} = \mathbf{0}$, $\boldsymbol{R}_d$ goes to $\mathbf{0}$ and $\boldsymbol{J}^+(\boldsymbol{\theta})$ cannot be calculated. However, the coordinate transformation gain of $\boldsymbol{\Phi}_{fb}(\boldsymbol{\theta}, \boldsymbol{e})$ does not also go to $\mathbf{0}$.

4 Derivation of Learning Result

4.1 Learning Model of the Neural Networks

The models proposed in this paper can serve as general learners which are C^1 class functions of the input vector. However, since it is difficult to show the convergence properties of the proposed learning model briefly [10], we will show them by using the learners which have a limited structure as follows:

$$\boldsymbol{\Phi}_{fb}(\boldsymbol{\theta}, \boldsymbol{e}) = \boldsymbol{\Psi}_{fb}(\boldsymbol{\theta})\boldsymbol{e} \quad (22)$$
$$\boldsymbol{\Phi}_{ff}(\boldsymbol{\theta}, \boldsymbol{\Delta x}_d) = \boldsymbol{\Psi}_{ff}(\boldsymbol{\theta})\boldsymbol{\Delta x}_d \quad (23)$$

where $\boldsymbol{\Psi}_{fb}(\boldsymbol{\theta}) \in \mathbf{R}^{m\times n}$ and $\boldsymbol{\Psi}_{ff}(\boldsymbol{\theta}) \in \mathbf{R}^{m\times n}$ are coordinate transformation gains that have learning parameters $\boldsymbol{W}_{fb} \in \boldsymbol{R}^{N_{fb}}$ and $\boldsymbol{W}_{ff} \in \boldsymbol{R}^{N_{ff}}$ respectively. For simplicity, we will show the convergence of

$$\boldsymbol{P}_{ff}(\boldsymbol{\theta}) = \boldsymbol{J}(\boldsymbol{\theta})\boldsymbol{\Psi}_{ff}(\boldsymbol{\theta}) \quad (24)$$

instead of $\boldsymbol{\Psi}_{ff}(\boldsymbol{\theta})$. Here, the change of $\boldsymbol{\Psi}(\boldsymbol{\theta}) = (\boldsymbol{\Psi}^T_{fb}(\boldsymbol{\theta}), \boldsymbol{P}^T_{ff}(\boldsymbol{\theta}))^T$ is considered.

Let $rs[\boldsymbol{S}]$ be the row string of the matrix $\boldsymbol{S}$. For simplicity, we assume that $\boldsymbol{W}_{fb}$ and $\boldsymbol{W}_{fb}$ are functions of $\boldsymbol{\theta}$ and the change of the coordinate transformation gains by the learning can be expressed as follows:

$$\boldsymbol{\Psi}^{(l+1)}(\boldsymbol{\theta}) = \boldsymbol{\Psi}^{(l)}(\boldsymbol{\theta}) + \eta\boldsymbol{\Delta\Psi}(\boldsymbol{\theta})$$
$$\boldsymbol{\Delta\Psi}(\boldsymbol{\theta}) = (\boldsymbol{\Delta\Psi}^T_{fb}(\boldsymbol{\theta}), \boldsymbol{\Delta P}^T_{ff}(\boldsymbol{\theta}))^T$$
$$rs[\boldsymbol{\Delta\Psi}_{fb}(\boldsymbol{\theta})] = rs[\boldsymbol{\Delta\Phi}_{fb}(\boldsymbol{\theta}, \boldsymbol{e})\boldsymbol{e}^T]\boldsymbol{\Omega}_{fb} \quad (25)$$
$$rs[\boldsymbol{\Delta P}_{ff}(\boldsymbol{\theta})] = rs[\boldsymbol{J}(\boldsymbol{\theta})\boldsymbol{\Delta\Phi}_{ff}(\boldsymbol{\theta}, \boldsymbol{\Delta x}_d)\boldsymbol{\Delta x}^T_d]\boldsymbol{\Omega}_{ff} \quad (26)$$

where $\boldsymbol{\Omega}_{fb} \in \mathbf{R}^{nm\times nm}$ and $\boldsymbol{\Omega}_{ff} \in \mathbf{R}^{nm\times nm}$ are positive definite matrices defined as:

$$\boldsymbol{\Omega}_{fb} = \sum_{j=1}^{N_{fb}} (\frac{\partial rs[\boldsymbol{\Psi}_{fb}(\boldsymbol{\theta})]}{\partial W_{fb(j)}})^T (\frac{\partial rs[\boldsymbol{\Psi}_{fb}(\boldsymbol{\theta})]}{\partial W_{fb(j)}}) \quad (27)$$
$$\boldsymbol{\Omega}_{ff} = \sum_{j=1}^{N_{ff}} (\frac{\partial rs[\boldsymbol{\Psi}_{ff}(\boldsymbol{\theta})]}{\partial W_{ff(j)}})^T (\frac{\partial rs[\boldsymbol{\Psi}_{ff}(\boldsymbol{\theta})]}{\partial W_{ff(j)}}). \quad (28)$$

η is an appropriate positive real number.

Let's consider the following matrix function.

$$\boldsymbol{F}(\boldsymbol{\theta}, \boldsymbol{\Psi}) = (\boldsymbol{F}^T_{fb}(\boldsymbol{\theta}, \boldsymbol{\Psi}), \boldsymbol{F}^T_{ff}(\boldsymbol{\theta}, \boldsymbol{\Psi}))^T \quad (29)$$
$$\boldsymbol{F}_{fb}(\boldsymbol{\theta}, \boldsymbol{\Psi}) = E[\boldsymbol{\Delta\Psi}_{fb}|\boldsymbol{\theta}] \quad (30)$$
$$\boldsymbol{F}_{ff}(\boldsymbol{\theta}, \boldsymbol{\Psi}) = E[\boldsymbol{\Delta P}_{ff}|\boldsymbol{\theta}]. \quad (31)$$

where $E[t(\boldsymbol{\theta})|\boldsymbol{\theta}]$ is the expected value of a scalar, a vector, or a matrix function $t(\boldsymbol{\theta})$ when the input vector is $\boldsymbol{\theta}$. Let $\boldsymbol{G}(\boldsymbol{\theta}, \boldsymbol{\Psi})$ be the Jacobian defined as follows:

$$\boldsymbol{G}(\boldsymbol{\theta}, \boldsymbol{\Psi}) = \frac{\partial rs[\boldsymbol{F}(\boldsymbol{\theta}, \boldsymbol{\Psi})]^T}{\partial rs[\boldsymbol{\Psi}]^T} = \begin{bmatrix} \boldsymbol{G}_{fb/fb}(\boldsymbol{\theta}) & \boldsymbol{G}_{fb/ff}(\boldsymbol{\theta}) \\ \boldsymbol{G}_{ff/fb}(\boldsymbol{\theta}) & \boldsymbol{G}_{ff/ff}(\boldsymbol{\theta}) \end{bmatrix}. \quad (32)$$

Let $\boldsymbol{\Psi}^+(\boldsymbol{\theta})$ be the learning result of $\boldsymbol{\Psi}(\boldsymbol{\theta})$ on which $\boldsymbol{\Psi}(\boldsymbol{\theta})$ finally converges by learning. If the equation

$$\boldsymbol{F}(\boldsymbol{\theta}, \boldsymbol{\Psi}^+(\boldsymbol{\theta})) \approx \mathbf{0} \quad (33)$$

is satisfied and the real components of all the eigenvalues of $\boldsymbol{G}(\boldsymbol{\theta}, \boldsymbol{\Psi}^+(\boldsymbol{\theta}))$ are negative, the learning result $\boldsymbol{\Psi}(\boldsymbol{\theta}) \approx \boldsymbol{\Psi}^+(\boldsymbol{\theta})$ is obtained when the initial status of $\boldsymbol{\Psi}(\boldsymbol{\theta})$ is appropriate [10]. When $\boldsymbol{d}(k)$ is not $\mathbf{0}$, we can obtain the following learning result by using Equation (12) or (21):

$$\boldsymbol{\Psi}^+(\boldsymbol{\theta}) = (\boldsymbol{J}^{+T}(\boldsymbol{\theta}), \boldsymbol{I}^T_n)^T. \quad (34)$$

Let $\boldsymbol{e}_\Psi(\boldsymbol{\theta})$ be the error matrix of the coordinate transformation gain defined as

$$\boldsymbol{e}_\Psi(\boldsymbol{\theta}) = (\boldsymbol{e}^T_{\Psi fb}(\boldsymbol{\theta}), \boldsymbol{e}^T_{Pff}(\boldsymbol{\theta}))^T = \boldsymbol{\Psi}^+(\boldsymbol{\theta}) - \boldsymbol{\Psi}(\boldsymbol{\theta}). \quad (35)$$

For simplicity, we will use $\boldsymbol{\Delta\Psi}^\#(\boldsymbol{\theta}, \boldsymbol{\Psi})$ defined as

$$\boldsymbol{\Delta\Psi}^\#(\boldsymbol{\theta}, \boldsymbol{\Psi}) = (\boldsymbol{\Delta\Psi}^{\#T}_{fb}(\boldsymbol{\theta}, \boldsymbol{\Psi}), \boldsymbol{\Delta P}^{\#T}_{ff}(\boldsymbol{\theta}, \boldsymbol{\Psi}))^T \quad (36)$$
$$\boldsymbol{\Delta\Psi}^\#_{fb}(\boldsymbol{\theta}, \boldsymbol{\Psi}) = E[\boldsymbol{\Delta\Phi}_{fb}(\boldsymbol{\theta}, \boldsymbol{e})\boldsymbol{e}^T|\boldsymbol{\theta}] \quad (37)$$
$$\boldsymbol{\Delta P}^\#_{ff}(\boldsymbol{\theta}, \boldsymbol{\Psi}) = \boldsymbol{J}(\boldsymbol{\theta})E[\boldsymbol{\Delta\Phi}_{ff}(\boldsymbol{\theta}, \boldsymbol{\Delta x}_d)\boldsymbol{\Delta x}^T_d|\boldsymbol{\theta}]. \quad (38)$$

The relationship between $\boldsymbol{\Delta\Psi}^\#(\boldsymbol{\theta}, \boldsymbol{\Psi})$ and $\boldsymbol{F}(\boldsymbol{\theta}, \boldsymbol{\Psi})$ is as follows:

$$rs[\boldsymbol{F}_{fb}(\boldsymbol{\theta}, \boldsymbol{\Psi})] = rs[\boldsymbol{\Delta\Psi}^\#_{fb}(\boldsymbol{\theta}, \boldsymbol{\Psi})]\boldsymbol{\Omega}_{fb} \quad (39)$$
$$rs[\boldsymbol{F}_{ff}(\boldsymbol{\theta}, \boldsymbol{\Psi})] = rs[\boldsymbol{\Delta P}^\#_{ff}(\boldsymbol{\theta}, \boldsymbol{\Psi})]\boldsymbol{\Omega}_{ff}. \quad (40)$$

4.2 Feed-forward Controller Learning

First, the convergence properties of the feed-forward controller learning expressed in Equation (5) is shown. For simplicity, $\boldsymbol{d}(k)$ is assumed to be a Gaussian noise vector. Since $\boldsymbol{d}(k)$ has no correlation with $\boldsymbol{\Delta x}_d(k)$,

$$E[\boldsymbol{e}(k-1)\boldsymbol{\Delta x}_d(k-1)|\boldsymbol{\theta}] = \boldsymbol{O}(\boldsymbol{e}_\Psi) \quad (41)$$

is obtained. $\boldsymbol{O}(\boldsymbol{e}_\Psi)$ is the sum of first and higher order terms of $\boldsymbol{e}_\Psi$ in each equation. If λ and is small enough,

$$\begin{aligned}&\boldsymbol{\Delta P}^{\#}_{ff}(\boldsymbol{\theta},\boldsymbol{\Psi}) = \boldsymbol{J}(\boldsymbol{\theta})E[\boldsymbol{\Delta\Phi}_{ff}(\boldsymbol{\theta},\boldsymbol{e})\boldsymbol{\Delta x}_d^T|\boldsymbol{\theta}]\\ &\approx \boldsymbol{J}(\boldsymbol{\theta})\boldsymbol{\Psi}_{fb}(\boldsymbol{\theta})\\ &\quad \boldsymbol{e}_{Pff}(\boldsymbol{\theta})E[\boldsymbol{\Delta x}_d\boldsymbol{\Delta x}_d^T|\boldsymbol{\theta}] + \boldsymbol{O}(\boldsymbol{e}_\Psi^2) \quad (42)\end{aligned}$$

is obtained by using Equation (8) and Equation (11). Therefore,

$$\boldsymbol{F}_{ff}(\boldsymbol{\theta},\boldsymbol{\Psi}^+) \approx \boldsymbol{0} \quad (43)$$

is established. The real components of all the eigenvalues of the following matrix

$$\boldsymbol{G}_{ff/ff}(\boldsymbol{\theta},\boldsymbol{\Psi}^+) = -(\boldsymbol{I}_n \otimes E[\boldsymbol{\Delta x}_d\boldsymbol{\Delta x}_d^T|\boldsymbol{\theta}])\boldsymbol{\Omega}_{ff} \quad (44)$$

are negative where $\otimes$ is a 2-operand operator that indicates the Kroneker product. $\boldsymbol{G}_{ff/fb}(\boldsymbol{\theta},\boldsymbol{\Psi}^+) = \partial rs[\boldsymbol{F}_{ff}(\boldsymbol{\theta},\boldsymbol{\Psi})]^T/\partial rs[\boldsymbol{\Psi}_{fb}]^T$ is $\boldsymbol{0}$. If $\boldsymbol{\Psi}_{fb}(\boldsymbol{\theta})$ converges on $\boldsymbol{J}^+(\boldsymbol{\theta})$, $\boldsymbol{P}_{ff}(\boldsymbol{\theta})$ approximately converges on the $n\times n$ identity matrix $\boldsymbol{I}_n$. Therefore, the feedback controller learning is essential.

4.3 Feedback Controller Learning

4.3.1 Learning based on Disturbance Noise

Here, the convergence properties of the feedback controller learning expressed in Equation (12) is shown. The error signal for the feedback controller can be approximated by

$$\begin{aligned}&\boldsymbol{\Delta\Phi}_{fb}(\boldsymbol{\theta}(k),\boldsymbol{e}(k))\\ &\approx -(\boldsymbol{I}_m - \boldsymbol{\Psi}_{fb}(\boldsymbol{\theta})\boldsymbol{J})(\boldsymbol{d}(k-1) + \boldsymbol{\Psi}_{fb}(\boldsymbol{\theta})\boldsymbol{e}(k-1))\\ &\quad +\boldsymbol{\Psi}_{fb}(\boldsymbol{\theta})\boldsymbol{e}_{Pff}\boldsymbol{\Delta x}_d(k-1). \quad (45)\end{aligned}$$

By using Equation (8) and (45), $\boldsymbol{\Delta\Psi}^{\#}_{fb}(\boldsymbol{\theta},\boldsymbol{\Psi})$ can be expressed as:

$$\begin{aligned}&\boldsymbol{\Delta\Psi}^{\#}_{fb}(\boldsymbol{\theta},\boldsymbol{\Psi}) \approx (\boldsymbol{I}_m - \boldsymbol{\Psi}_{fb}(\boldsymbol{\theta})\boldsymbol{J}(\boldsymbol{\theta}))\boldsymbol{R}_d\boldsymbol{J}^T(\underline{\mathrm{m}}\theta)\\ &\quad +\boldsymbol{\Psi}_{fb}\boldsymbol{e}_{Pff}E[\boldsymbol{\Delta x}_d(k-1)\boldsymbol{e}^T(k)|\boldsymbol{\theta}]\\ &\quad -\boldsymbol{\Psi}_{fb}(\boldsymbol{\theta})\boldsymbol{J}(\boldsymbol{\theta})\boldsymbol{e}_{\Psi fb}(\boldsymbol{\theta})\\ &\quad\quad E[e(k-1)\boldsymbol{e}^T(k-1)|\boldsymbol{\theta}](\boldsymbol{J}(\boldsymbol{\theta})\boldsymbol{e}_{\Psi fb}(\boldsymbol{\theta}))^T\\ &= (\boldsymbol{I}_m - \boldsymbol{\Psi}_{fb}(\boldsymbol{\theta})\boldsymbol{J}(\boldsymbol{\theta}))\boldsymbol{R}_d\boldsymbol{J}^T(\underline{\mathrm{m}}\theta) + \boldsymbol{O}(\boldsymbol{e}_\Psi^2). \quad (46)\end{aligned}$$

Equation (33) is clearly satisfied.

$$\boldsymbol{G}_{fb/fb}(\boldsymbol{\theta},\boldsymbol{\Psi}^+) = -(\boldsymbol{I}_m \otimes (\boldsymbol{J}(\boldsymbol{\theta})\boldsymbol{R}_d\boldsymbol{J}^T(\boldsymbol{\theta})))\boldsymbol{\Omega}_{fb} \quad (47)$$

is obtained. Since the real components of all the eigenvalues of $\boldsymbol{G}_{fb/fb}(\boldsymbol{\theta},\boldsymbol{\Psi}^+)$ and $\boldsymbol{G}_{ff/ff}(\boldsymbol{\theta},\boldsymbol{\Psi}^+)$ are negative and $\boldsymbol{G}_{ff/fb}(\boldsymbol{\theta},\boldsymbol{\Psi}^+)$ is $\boldsymbol{0}$ as shown in Equation (42), the real components of all the eigenvalues of $\boldsymbol{G}(\boldsymbol{\theta},\boldsymbol{\Psi}^+(\boldsymbol{\theta}))$ are negative. Therefore, Equation (14) is obtained by the learning based on the disturbance noise.

4.3.2 Learning based on Disturbance Noise and Feedback Error Signal

Here, the convergence properties of the feedback controller learning expressed in Equation (21) is shown. By using Equation (8) and Equation (19),

$$\begin{aligned}&\boldsymbol{\Delta\Psi}^{\#}_{fb}(\boldsymbol{\theta},\boldsymbol{\Psi}) \approx (\boldsymbol{I}_m - \boldsymbol{\Psi}_{fb}\boldsymbol{J})\\ &\quad(\boldsymbol{R}_d\boldsymbol{J}^T + \boldsymbol{\Psi}_{fb}E[\boldsymbol{e}(k-1)\boldsymbol{e}^T(k-1)|\boldsymbol{\theta}])\\ &\quad\quad +\boldsymbol{O}(\boldsymbol{e}_\Psi^2(\boldsymbol{\theta}))\\ &= (\boldsymbol{I}_m - \boldsymbol{\Psi}_{fb}(\boldsymbol{\theta})\boldsymbol{J}(\boldsymbol{\theta}))(\boldsymbol{I}_m + \boldsymbol{\Psi}_{fb}(\boldsymbol{\theta})\boldsymbol{J}(\boldsymbol{\theta}))\\ &\quad\quad \boldsymbol{R}_d\boldsymbol{J}^T(\boldsymbol{\theta}) + \boldsymbol{O}(\boldsymbol{e}_\Psi^2(\boldsymbol{\theta})) \quad (48)\end{aligned}$$

is obtained. Equation (33) is clearly satisfied.

$$\begin{aligned}&\boldsymbol{G}_{fb/fb}(\boldsymbol{\theta},\boldsymbol{\Psi}^+) = -((\boldsymbol{I}_m + \boldsymbol{J}^+(\boldsymbol{\theta})\boldsymbol{J}(\boldsymbol{\theta}))^T\\ &\quad\quad \otimes(\boldsymbol{J}(\boldsymbol{\theta})\boldsymbol{R}_d\boldsymbol{J}^T(\boldsymbol{\theta})))\boldsymbol{\Omega}_{fb} \quad (49)\end{aligned}$$

is obtained. Since the real components of all the eigenvalues of $\boldsymbol{G}_{fb/fb}(\boldsymbol{\theta},\boldsymbol{\Psi}^+)$ and $\boldsymbol{G}_{ff/ff}(\boldsymbol{\theta},\boldsymbol{\Psi}^+)$ are negative, the real components of all the eigenvalues of $\boldsymbol{G}(\boldsymbol{\theta},\boldsymbol{\Psi}^+(\boldsymbol{\theta}))$ are negative. Therefore, the learning result expressed in Equation (14) is obtained by the proposed learning method.

When $\boldsymbol{d}(k)$ is $\boldsymbol{0}$, the learning result has not been obtained yet. However, since $E[\boldsymbol{e}(k-1)\boldsymbol{e}^T(k-1)|\boldsymbol{\theta}]$ in Equation (48) does not go to $\boldsymbol{0}$ even when $\boldsymbol{d}(k)$ is $\boldsymbol{0}$, $\boldsymbol{\Psi}_{fb}(\boldsymbol{\theta})$ does not also go to $\boldsymbol{0}$. The feedback controller $\boldsymbol{\Phi}_{fb}(\boldsymbol{\theta},\boldsymbol{e})$ still keeps the coordinate transformation function.

5 Numerical Simulations

5.1 Coordinate Transformation Learning of 3 DOF arm

Numerical simulation experiments were performed in order to evaluate the performance of the proposed model. The inverse kinematics of a 3 DOF arm moving on a 2 DOF plane were considered. The relationship between the joint angle vector $\boldsymbol{\theta} = (\theta_1,\theta_2,\theta_3)^T$ and the hand position vector $\boldsymbol{x} = (x,y)^T$ was defined as:

$$x = x_0 + L_1\cos(\theta_1) + L_2\cos(\theta_1+\theta_2) + L_3\cos(\theta_1+\theta_2+\theta_3) \quad (50)$$

$$y = y_0 + L_1\sin(\theta_1) + L_2\sin(\theta_1+\theta_2) + L_3\sin(\theta_1+\theta_2+\theta_3). \quad (51)$$

The range for θ_1 was $(-30°, 120°)$; the range for θ_2 was $(0°, 120°)$; and the range for θ_3 was $(-75°, 75°)$. L_1 was 0.30 m, L_2 was 0.25 m and L_3 was 0.15 m.

Random straight lines provided the desired trajectories for the hand. T was 20 and γ is 1.0. The tracking control trials expressed as Equation (3) with online incremental learning were performed. The simulation used two artificial neural networks with four layers. The first layer had 5 units and the forth layer had 3 units. The other layers had 15 units each. The first layer and the forth layer consisted of linear units. The second layer and the third layer consisted of sigmoid units. It is highly unlikely that the human nervous system utilizes the back-propagation learning method. However, since the choice of the learning method of the neural networks is not essential for the evaluation of the proposed learning model, back-propagation learning was used.

When the hand position error grew larger than $0.2m$, or two joints reach their joint limits, the trial was regarded as a failure and tracking control was given up. The standard deviation of each component of $\boldsymbol{d}(k)$ was 0.05. Learning based on Equations (5) and (21) was conducted 20 times in one tracking trial. 1,000 tracking trials were conducted to estimate the RMS (Root Mean Square) error. λ and λ_{fb} were set at 0.001.

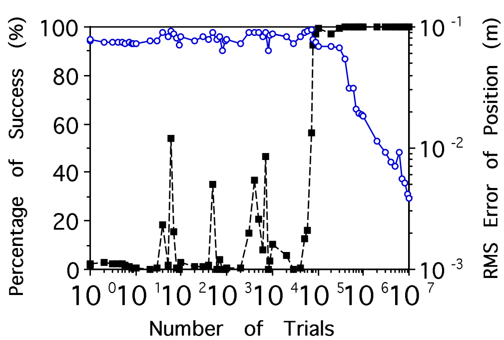

The solid line with white circles shows RMS Error (m). The dashed line with black boxes shows percentage of successful trials (%).

Fig. 5: Learning Process of 3-DOF Arm Controller

Fig. 5 shows the progress of the proposed learning model. The percentage of the successful tracking trials increases and the RMS error decreases as the number of trials increases. Fig. 6 illustrates an example of tracking control to a straight line by the controller after 2×10^7 learning trials.

In order to evaluate the influence of having no disturbance noise, $\boldsymbol{d}(k)$ was set at $\mathbf{0}$ and learning continued for 10^7 more trials. The RMS error became $1.40 \times 10^{-2}(m)$. The performance of the controller deteriorated only slightly. When the learning rule (12) was used, the percentage of successful trials decreased 25% and the RMS error increased 4.5×10^{-2}. The proposed learning model can keep the coordinate transformation function when $\boldsymbol{d}(k)$ is $\mathbf{0}$.

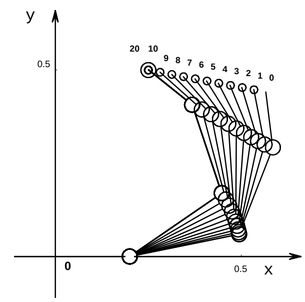

Fig. 6: One Example of Tracking Control

5.2 Coordinate transformation learning of a 7 DOF arm

We performed simulations of the coordinate transformation learning of the feedback controller of a human-like 7-DOF arm as shown in Fig. 7. The arm length was $0.755m$

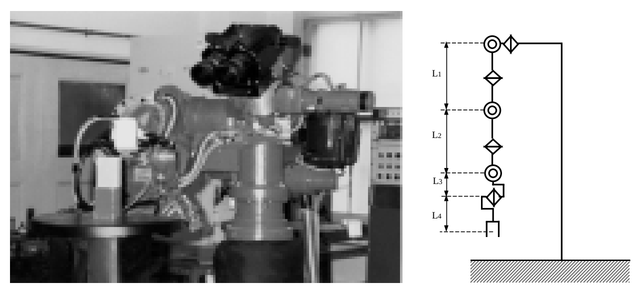

Fig. 7: TELE-existence Slave ARm II (TELESAR II)

In order to accelerate the learning, neural networks that have a structure suitable for the coordinate transformation as shown in Equation (22) were used. The desired output signal for the coordinate transformation gain of the feedback controller $\boldsymbol{\Psi}'_{fb}(\boldsymbol{\theta})$ was expressed as follows:

$$\boldsymbol{\Psi}'_{fb}(\boldsymbol{\theta}) = \boldsymbol{\Psi}_{fb}(\boldsymbol{\theta}) + \frac{(\boldsymbol{\Phi}'_{fb}(\boldsymbol{\theta},\boldsymbol{e}) - \boldsymbol{\Phi}_{fb}(\boldsymbol{\theta},\boldsymbol{e}))\boldsymbol{e}^T}{0.05 + |\boldsymbol{e}||\boldsymbol{\Phi}'_{fb}(\boldsymbol{\theta},\boldsymbol{e})|} \quad (52)$$

$\boldsymbol{\Psi}_{ff}(\boldsymbol{\theta})$ was also updated in the same manner described in the above equation.

The first layer of the coordinate transformation gains had 7 linear units and the forth layer had 21 units. The other layers had 25 sigmoid units each. 16384 tracking trials were conducted to estimate the RMS error. λ and λ_{fb} were set at 0.01. Fig. 8 shows the progress of the proposed learning model. We concluded that the proposed learning model succeeded in the coordinate transformation learning of the 7-DOF arm.

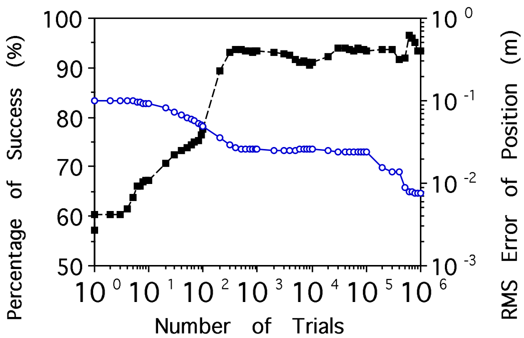

Fig. 8: Learning Process of 7-DOF Arm Controller

6 Conclusions

A learning model of coordinate transformation of the hand position feedback controller based on disturbance noise and the feedback error signal was proposed and tested in this paper. The desired output signal of the proposed learning model can be calculated by the linear combination of the control signals. The proposed model is capable of coordinate transformation learning without using a forward model or complex signal switching. Modified learning models considering the time delay in the vision system will be reported in the near future.

References

[1] T. Ogino and S. Ishii, "Long-term Results after Pollicization for Congenital Hand Deformities," *Hand Surgery 2*(2), pp. 79-85, 1997.

[2] M. Kuperstein, "Neural Model of Adaptive Hand-Eye Coordination for Single Postures," *Science*, 239, pp.1308-1311, 1988.

[3] M. I. Jordan and D. E. Rumelhart, "Forward Models: Supervised Learning with a Distal Teacher," *Cognitive Science*, 16, 307-354, 1992.

[4] F. H. Guenther and D. M. Barreca, "Neural Models for Flexible Control of Redundant Systems," in P. Morasso and V. Sanguineti (Eds.), *Self-organization, Computational Maps, and Motor Control*, Elsevier, pp. 383-421, 1997.

[5] M. A. Arbib, "I.3. Dynamics and Adaptation in Neural Networks", in M. A. Arbib (Ed.), *The Handbook of Brain Theory and Neural Networks*, The MIT Press, pp.17-25, 1995.

[6] M. Kawato, K. Furukawa and R. Suzuki, "A Hierarchical Neural-network Model for Control and Learning of Voluntary Movement," *Biological Cybernetics,* 57, pp. 169-185, 1987.

[7] E. Oyama and S. Tachi, "A Study of Human Hand Position Control Learning: Output Feedback Inverse Model," *Proc. of IJCNN 1991 Singapore*, pp. 1434-1443, 1991.

[8] E. Oyama and S. Tachi, "Coordinate Transformation Learning of Hand Position Feedback Controller by Using Change of Position Error Norm," *Advances in Neural Information Processing Systems 11*, pp. 1038-1044, 1999.

[9] E. Oyama, T. Maeda and S. Tachi, "Coordinate Transformation Learning of Hand Position Feedback Controller based on Disturbance Noise and Feedback Error Signal," *Proc. of IJCNN 2000 Como*, 2000.

[10] E. Oyama, "Human Coordinate Transformation Learning Models of Hand Position Feedback Controller," Ph.D. Thesis, School of Engineering, The University of Tokyo, 2000.

[11] M. Kawai, "Development of Reaching Behavior from 9 to 36 Months," *Japanese Psychological Research*, Vol.29, pp.184-190, 1987.

[12] E. Thelen and L. B. Smith, *A Dynamic Systems Approach to the Development of Cognition and Action*, The MIT Press, 1994.

[13] P. H. Clammam,"Statical Analysis of Motor Unit Firing Patterns in Human Skeletal Muscle," *Biophysics Journal*, Vol. 9. pp.1233-1251,1969.

[14] P. B. C. Matthews, "Relationship of Firing Intervals of Human Motor Units to the Trajectory of Post-spike After-hyperpolarization and Synaptic Noise," *Journal of Physiology*, Vol.492, pp.597-628, 1996.

[15] C. M. Harris and D. M. Wolpert, "Signal-dependent noise determines motor planning," *Nature*, Vol.394, pp.780-784, 1998.

[16] K. Nakamura, "A Theory of Cerebral Learning Regulated by the Reward System: I. Hypotheses and Mathematical Description," *Biological Cybernetics*, Vol.68, pp.491-498, 1993.

[17] O. Lippold, "Phisiological Tremor, " *Scientific American*, Vol.224, pp. 67-73, 1971.

[18] D. T. McRuer and H. R. Jex,"A Review of Quasi-Linear Pilot Models," *IEEE Trans. on Human Factors in Electronics*, HFE-8, 3, pp. 38-51, 1963